Reaction of Aspartate Aminotransferase with L-*erythro*-3-Hydroxyaspartate: Involvement of Tyr70 in Stabilization of the Catalytic Intermediates†

Hideyuki Hayashi and Hiroyuki Kagamiyama*

Department of Biochemistry, Osaka Medical College, Takatsuki, Osaka 569, Japan

Received February 2, 1995; Revised Manuscript Received May 1, 1995⊗

ABSTRACT: The reaction of *Escherichia coli* aspartate aminotransferase (AspAT) with L-*erythro*-3-hydroxyaspartate (HOAsp) produces an intense absorption at 494 nm (ϵ = 13 650 M^{-1} cm^{-1}), which is ascribed to the quinonoid intermediate. However, when Tyr70 of AspAT has been replaced by Phe, the enzyme shows only a faint absorption at 494 nm (ϵ = 522 M^{-1} cm^{-1}) on the reaction with HOAsp. This indicates the involvement of the hydroxy group of Tyr70 in stabilizing the quinonoid intermediate formed from HOAsp and pyridoxal 5′-phosphate at the AspAT active site. Kinetic analysis of the absorption changes of the wild-type and Y70F mutant AspATs has shown that the reactions with HOAsp conform to the equation, $E_L + S \rightleftarrows ES_1 \rightleftarrows ES_2 \rightleftarrows ES_3 \rightleftarrows E_M + P$, in which there is a rapid formation of the quinonoid intermediate (ES_2) from ES_1, followed by a slow equilibrium between ES_2 and ES_3. ES_3 absorbs primarily at 330 nm. The kinetic parameters for individual steps have been determined, and free energy profiles for the reactions of the two enzymes with HOAsp have been obtained. The stability of the quinonoid intermediates of the two enzymes in the normal catalytic reactions with aspartate has been assessed by static measurement of the spectra in the presence of both aspartate and oxalacetate, and the free energy profiles for the reactions have been similarly obtained. Comparison of the free energy levels in the profiles showed that the interaction of the β-hydroxy group of HOAsp with the hydroxy group of Tyr70 accounts for 8.7 kJ mol^{-1} of the 18.5 kJ mol^{-1} stabilization of the quinonoid intermediate by the β-hydroxy group. Model building of the active site of AspAT complexed with HOAsp suggests that the rest of the stabilization is mediated through the interaction of the β-hydroxy group of HOAsp with the protonated ϵ-amino group of Lys258. This interaction is expected to strengthen the hydrogen-bonding network involving Tyr70, HOAsp, and the coenzyme phosphate. A similar network is possibly formed in the carbinolamine intermediate, suggesting ES_3 to be the carbinolamine. A mechanism for the reaction of AspAT with HOAsp, which conforms to all the kinetic and spectroscopic data presented here, is proposed. This study provides a basis for subsequent spectroscopic characterization of the HOAsp−AspAT complex, which is a good model for the critical intermediate (quinonoid) structure of the AspAT-catalyzed reactions.

Aspartate aminotransferase (AspAT)[1] is a pyridoxal 5′-phosphate (PLP)-dependent enzyme which catalyzes the reversible transfer of the amino group of aspartate to 2-oxoglutarate to form oxalacetate and glutamate by the following ping-pong Bi Bi mechanism:

$$\text{aspartate} + E_L \rightleftarrows \text{oxalacetate} + E_M$$

$$\text{glutamate} + E_L \rightleftarrows \text{2-oxoglutarate} + E_M$$

where E_L and E_M in each half-reaction denote the PLP form and the pyridoxamine 5′-phosphate (PMP) form of the enzyme, respectively. The three-dimensional structures have been solved for both the mitochondrial and cytosolic isoenzymes (Arnone et al., 1985b; Jansonius et al., 1985) and the *Escherichia coli* enzyme (Danishevsky et al., 1990; Kamitori et al., 1991; Jäger et al., 1994; Okamoto et al., 1994). The enzyme is a dimer of identical subunits, each containing one active site located near the subunit interface. The aldehyde group of PLP forms a Schiff base to the ϵ-amino group of Lys258.[2] In addition, the phosphate group of PLP electrostatically interacts with the guanidinium group of Arg266 and makes hydrogen bonds to the hydroxy groups of Ser296 and Tyr70. On the basis of the kinetic, spectroscopic, and crystallographic studies, a detailed mechanism of the action of AspAT has been proposed (Kirsch et al., 1984; Arnone et al., 1985a). The half-reaction (Scheme 1) consists of the following steps: association of the amino acid substrate and E_L to form the Michaelis complex; transaldimination from the PLP−Lys258 aldimine to the PLP−substrate aldimine (external aldimine) via a geminal diamine intermediate; deprotonation at C^{α} of the PLP−substrate aldimine to form the quinonoid intermediate; reprotonation at C4′ to form the ketimine; hydrolysis of the ketimine via a carbinolamine intermediate; dissociation of the Michaelis complex to the oxo acid product and E_M. Most of the intermediates formed during the reaction, such as the

† This work was supported by Grant-in-Aids (06680628 to H.H. and 14454160 to H.K.) from the Ministry of Education, Science, and Culture of Japan.

* Author to whom correspondence should be addressed.

⊗ Abstract published in *Advance ACS Abstracts,* July 1, 1995.

[1] Abbreviations: AspAT, aspartate aminotransferase (EC 2.6.1.1); PLP, pyridoxal 5′-phosphate; PMP, pyridoxamine 5′-phosphate; HOAsp, L-*erythro*-3-hydroxyaspartate; OG, oxaloglycolate (2-hydroxy-3-oxobutanedioate); Asp, aspartate; OA, oxalacetate; HEPES, *N*-(2-hydroxyethyl)piperazine-*N*′-(2-ethanesulfonic acid); WT AspAT, wild-type AspAT; Y70F AspAT, AspAT in which the residue Tyr70 was replaced by a phenylalanine residue.

[2] The amino acid residue is numbered according to the sequence of pig cytosolic aspartate aminotransferase (Ovchinnikov et al., 1973).

0006-2960/95/0434-9413$09.00/0

Scheme 1: Reaction Mechanism of Aspartate Aminotransferase[a]

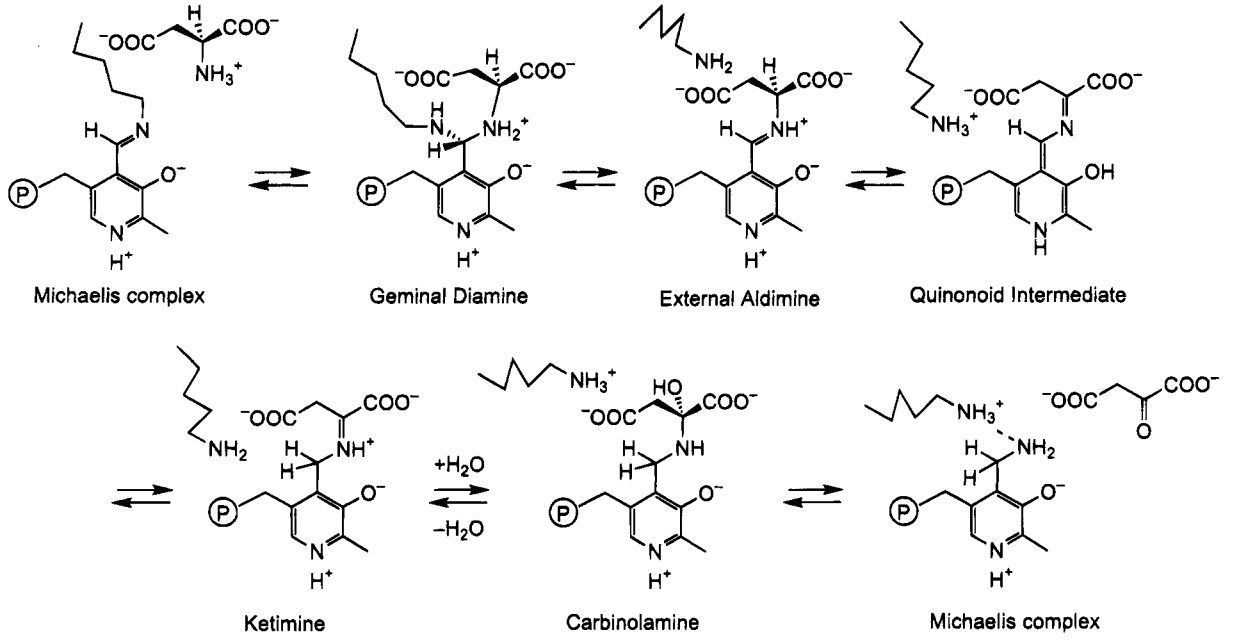

[a] The intermediates for the reaction asparatate + $E_L \rightleftharpoons$ oxalacetate + E_M are shown. In E_L, the aldehyde group of PLP forms a Schiff base with the ϵ-amino group of Lys258 (the internal aldimine). In the external aldimine, the substrate aspartate forms a Schiff base with PLP and the side chain of Lys258 is expelled. The deprotonated ϵ-amino group of Lys258 is supposed to be the base that catalyzes the tautomerization between the external aldimine and the ketimine, and hydrolysis of the ketimine.

Michaelis complexes, the PLP−substrate aldimine, and the ketimine, have been extensively characterized by the use of substrate analogs and natural substrates (Kirsch et al., 1984; Arnone et al., 1985a,b; Jansonius et al., 1985; Malashkevich et al., 1993). However, the quinonoid intermediate has been less extensively investigated despite the fact that its stabilization through the interaction with the surrounding AspAT residues is a crucial chemical event during the enzymatic transamination reaction (Kirsch et al., 1984; Arnone et al., 1985a). This is mainly because the quinonoid intermediate is only transiently formed during the normal catalytic reaction (Metzler & Metzler, 1987).

L-*erythro*-3-Hydroxyaspartate (HOAsp) has been shown by Jenkins (1961) that it produces an intense absorption at 492 nm when reacting with pig cytosolic AspAT, indicating the production of the quinonoid intermediate. Therefore, the HOAsp−AspAT complex absorbing at 490−500 nm could be a good model for the quinonoid intermediate of the reaction of AspAT with aspartate. Characterization of the structure of the HOAsp−AspAT complex has been therefore required, because it would provide a basis for subsequent spectroscopic and X-ray crystallographic analyses on this complex. However, unlike succinate and 2-methylaspartate, which are analogs that form Michaelis complex and the external aldimine (Scheme 1), respectively, the chemical structure of HOAsp does not allow one to anticipate that the reaction stops at the quinonoid intermediate, and there had been no satisfactory explanation for the accumulation of the quinonoid species (Kirsch et al., 1984; Arnone et al., 1985a,b; Jansonius et al., 1985). Recently, Taylor and Metzler (1990) suggested that the β-hydroxy O of HOAsp can form a hydrogen bond with the phenolic hydroxy O (O^{η}) of Tyr70 when the quinonoid intermediate was modeled in the active site of pig cytosolic AspAT. The O^{η} atom of Tyr70, on the other hand, appears to form hydrogen bonds to both the phosphate O of PLP and the ϵ-amino N(N^{ζ}) of Lys258 (Arnone et al., 1985b; Jansonius et al., 1985). To clarify the involvement of the β-hydroxy group of HOAsp and the phenolic hydroxy group of Tyr70 in the above hydrogen-bonding network is therefore of great importance in discussing the structure of the quinonoid intermediate produced by HOAsp and AspAT. In this study, we analyzed the reactions of HOAsp with both the wild-type (WT) and Y70F mutant enzymes, compared them to the reactions with aspartate, and studied the factor(s) stabilizing the quinonoid structure formed during the course of the transamination reaction.

MATERIALS AND METHODS

Chemicals. Dihydroxyfumaric acid was obtained from Aldrich (Milwaukee, WI). Aspartic acid and oxalacetic acid were from Nacalai Tesque (Kyoto, Japan). L-*erythro*-3-Hydroxyaspartic acid was synthesized as described by Harruff and Jenkins (1978). The wild-type (WT) and Y70F AspATs were prepared as described previously (Kuramitsu et al., 1990; Inoue et al., 1991). All other chemicals were of the highest grade commercially available.

Determination of Protein Concentration. For both WT and Y70F AspATs, the concentration of the enzyme subunit in solution was determined spectrophotometrically as described previously (Kuramitsu et al., 1990; Inoue et al., 1991). The apparent molar extinction coefficient $\epsilon = 4.7 \times 10^4\ M^{-1}\ cm^{-1}$ was used for the PLP form of both enzymes at 280 nm.

Spectrophotometric Measurements. Absorption spectra were measured using a Hitachi U-3300 spectrophotometer at 25 °C and pH 8.0. The buffer solution for the absorption measurements contained 50 mM HEPES−NaOH as a buffer component and 0.1 M KCl. Protein concentrations were generally 20−50 μM. Resolution of the spectra into components with lognormal curves (Metzler & Metzler, 1987) were performed using PeakFit (Jandel Scientific, San

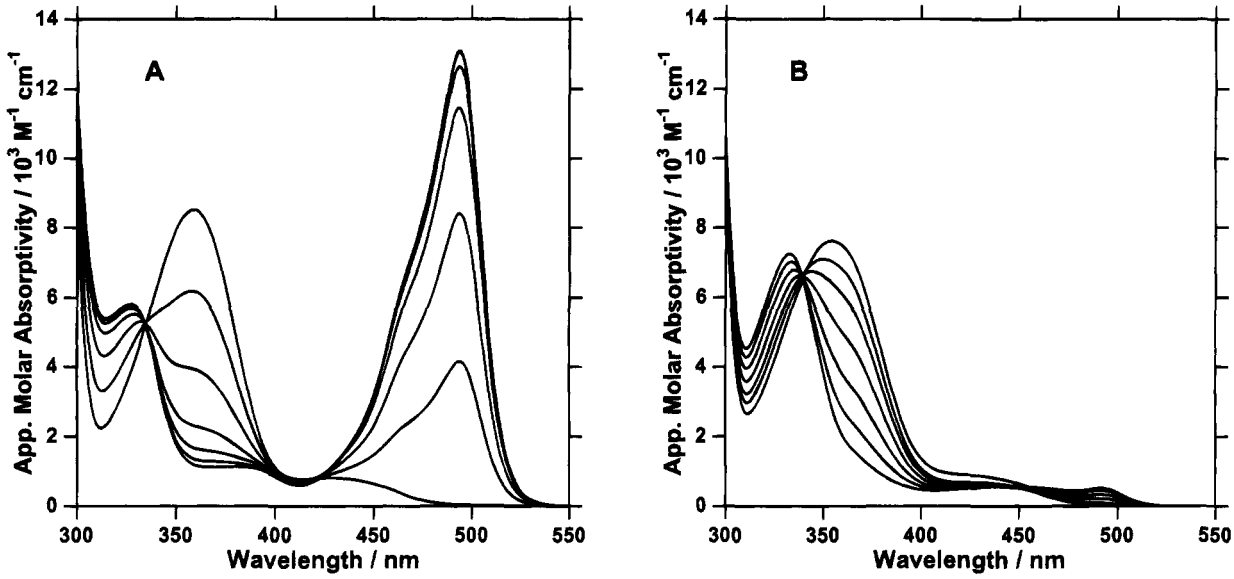

FIGURE 1: Absorption spectra of WT AspAT (A) and Y70F AspAT (B) in the presence of various concentrations of HOAsp. Spectra were taken at 25 °C in 50 mM HEPES−NaOH buffer, pH 8.0, containing 0.1 M KCl, with 43.5 μM enzymes. In each panel, the total concentrations of HOAsp added are (from bottom to top of the 494-nm peak): 0, 0.0498, 0.148, 0.385, 0.861, 1.80, and 4.07 mM. In panel A, the spectrum with 1.80 mM HOAsp and that with 4.07 mM HOAsp were almost superimposable.

Rafael, CA). The values reported by Metzler and Metzler (1987) of the skewness (ϱ) of individual absorption components were used in the analysis.

Rapid reactions were analyzed using a Union Giken RA-401 stopped-flow spectrophotometer. The dead time for this system was estimated by plotting the logarithm for the amplitude of the absorption changes of the reduction of 2,6-dichlorophenolindophenol by ascorbic acid against the rate constant (Tonomura et al., 1978) just before and after a series of measurements, and was used for calibrating the absorption changes during the dead time. The values were generally around 1.5 ms under a pressure of 500 kPa. The absorbance was digitized and recorded for 250 points at regular intervals within the selected time scale, and the points were subjected to exponential curve fitting using IGOR (WaveMetrics, Lake Oswego, OR).

RESULTS

Reaction of WT AspAT with HOAsp. The spectra of WT AspAT in the presence of various concentrations of HOAsp are shown in Figure 1A. WT AspAT has an absorption band at 358 nm, which represents the deprotonated aldimine structure of the PLP−Lys258 Schiff base (Kallen et al., 1985). HOAsp diminished the absorption band at 358 nm and produced an intense absorption band at 494 nm and a weaker one at 330 nm in a concentration-dependent manner. The absorption band at around 490−500 nm is generally ascribed to the quinonoid intermediates (for the structure, see Scheme 1). When the reaction of WT AspAT with HOAsp was followed in a stopped-flow spectrophotometer, a rapid increase in absorbance at 494 nm and a slow decrease in the absorbance were observed (Figure 2). These results are essentially identical with those reported for the reaction of pig cytosolic AspAT by Hammes and Haslam (1969) and Harruff and Jenkins (1978), who showed that the reaction can be analyzed by assuming the following reaction scheme:

$$E_L + S \overset{K_S^{Am}}{\rightleftharpoons} ES_1 \underset{k_{-2}}{\overset{k_{+2}}{\rightleftharpoons}} ES_2 \underset{k_{-3}}{\overset{k_{+3}}{\rightleftharpoons}} ES_3 \qquad (1)$$

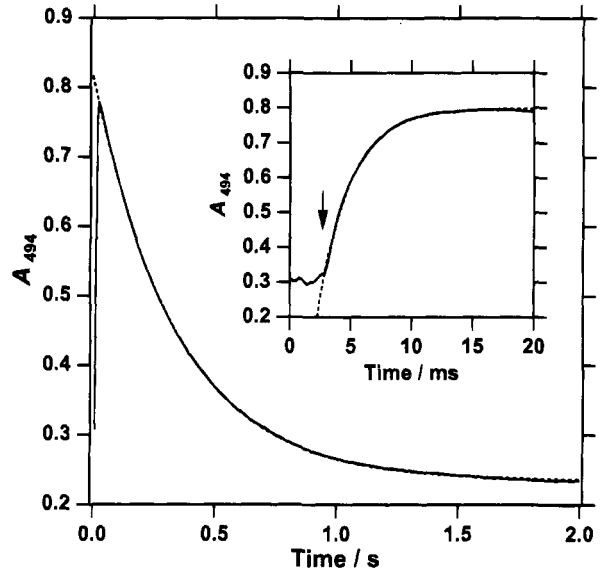

FIGURE 2: Absorption changes during the reaction of WT AspAT with HOAsp. The reaction was started in a stopped-flow spectrophotometer by mixing 20.0 μM enzyme with 2.0 mM HOAsp in 50 mM HEPES−NaOH buffer, pH 8.0, containing 0.1 M KCl at 25 °C. The reaction was monitored at 494 nm with time scales of 20 ms and 2 s. The progress curve with a time scale of 20 ms is shown in the inset, and the arrow indicates the point at which the flow was stopped. The A_{494} value of zero was set arbitrarily. The dashed curve in each panel is an exponential curve to which the data were fit.

where S is the substrate amino acid (in this case HOAsp), K_S^{Am} is the dissociation constant for the ES_1 complex, and k_{+2}, k_{-2}, k_{+3}, and k_{-3} are the rate constants for individual reactions. In this scheme, ES_2 is the species responsible for the absorption at 492 nm, and its rapid formation from ES_1 and slow conversion to ES_3 are considered to account for the observed biphasic changes in the absorption at 492 nm. Dissociation of ES_3 into oxaloglycolate (OG; 2-hydroxy-3-oxobutanedioate) and the PMP form of the enzyme (E_M) was neglected. This was because OG has such a high affinity with E_M that virtually none of the E_M is produced when high

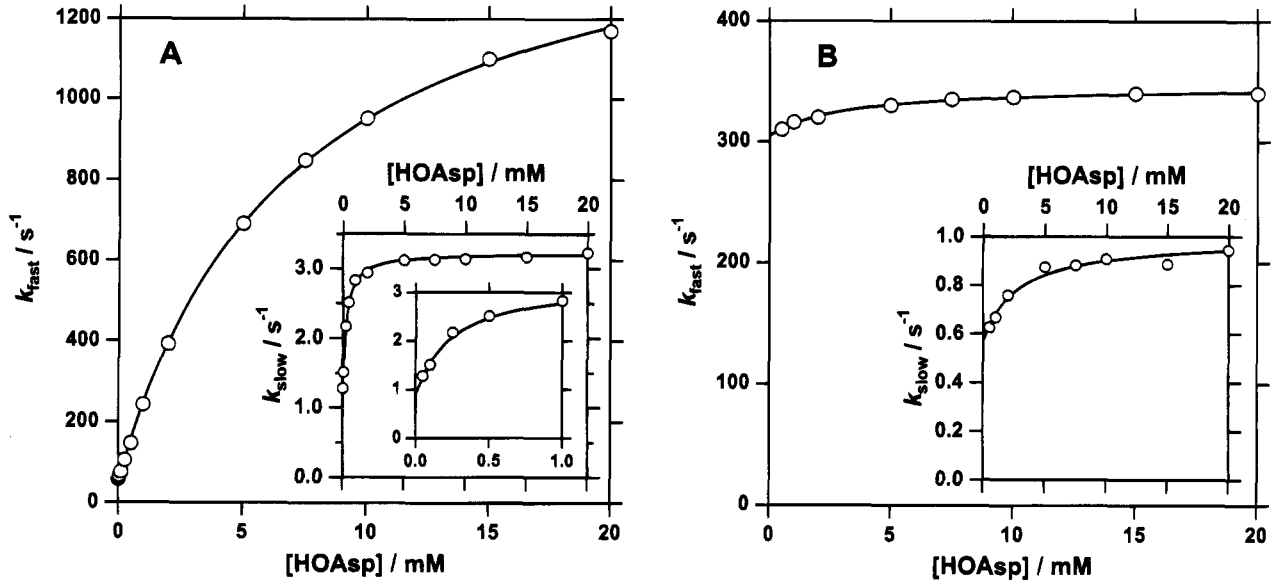

FIGURE 3: Dependency of the apparent rate constants for the fast phase and the slow phase reactions (Figure 2) on the HOAsp concentration. WT AspAT (20.0 μM) and Y70F AspAT (40.0 μM) were reacted with the indicated concentrations of HOAsp. The apparent rate constants for the fast and slow phases were obtained by fitting the data of the absorption changes to the exponential curves as shown in Figure 2 and were plotted versus the HOAsp concentrations. (A) WT AspAT; (B) Y70F AspAT. In each panel, the data for the slow phase rate constants are shown in the inset. The inset in the inset of (A) shows the expansion of the points for low concentrations of HOAsp. The solid curves were determined by fitting the data to eqs 3 and 4. The reactions of Y70F AspAT were measured in the presence of 5 mM dihydroxyfumarate.

concentrations of enzyme were reacted with HOAsp (Harruff & Jenkins, 1978). If we take into account the dissociation of OG from E_M, the complete reaction scheme is the same as that for the transamination half-reaction of normal substrates (Fasella & Hammes, 1967):

$$E_L + S \overset{K_S^{Am}}{\rightleftharpoons} ES_1 \underset{k_{-2}}{\overset{k_{+2}}{\rightleftharpoons}} ES_2 \underset{k_{-3}}{\overset{k_{+3}}{\rightleftharpoons}} ES_3 \overset{K_S^{Ox}}{\rightleftharpoons} E_M + P \quad (2)$$

Here P denotes the oxo acid corresponding to the amino acid S, and K_S^{Ox} is the dissociation constant for the ES_3 complex. We can expect that the addition of P prevents the dissociation of ES_3 into E_M and P, thereby increasing the concentration of the intermediates. Then we carried out the reaction of HOAsp with WT AspAT in the presence and absence of dihydroxyfumarate, an enol tautomer of OG which readily tautomerizes to OG in aqueous solutions. The addition of dihydroxyfumarate changed neither the absorption at 494 nm nor the apparent rate constants for the absorption changes shown in Figure 2 (data not shown). This indicated that the dissociation of ES_3 into E_M and P is negligible for the reaction of WT AspAT with HOAsp, if we used enzyme concentrations as high as 20 μM, and the reactions can be analyzed within the framework of eq 1.

Based on eq 1 and the observation that the two reaction phases are well separated on the time axis (Figure 2), the apparent rate constants for the fast phase (rapid increase in A_{494}) and the slow phase (slow decrease in A_{494}) can be expressed using the kinetic parameters shown in eq 1 as follows (Hammes & Schimmel, 1966, 1970).[3]

$$k_{fast} = k_{+2}\frac{[S]}{K_S^{Am} + [S]} + k_{-2} \quad (3)$$

$$k_{slow} = k_{+3}\frac{k_{+2}}{k_{+2} + k_{-2}}\frac{[S]}{[k_{-2}/(k_{+2} + k_{-2})]K_S^{Am} + [S]} + k_{-3} \quad (4)$$

The apparent rate constants for both phases clearly showed saturation kinetics (Figure 3A). The kinetic parameters in eq 1 were obtained by fitting the data of Figure 3A to eqs 3 and 4. The values are as follows: $K_S^{Am} = 6.87 \pm 0.16$ mM, $k_{+2} = 1510 \pm 13$ s^{-1}, $k_{-2} = 53.2 \pm 2.5$ s^{-1}, $k_{+3} = 2.42 \pm 0.05$ s^{-1}, and $k_{-3} = 0.894 \pm 0.042$ s^{-1}.

When the reaction of WT AspAT with HOAsp was monitored at wavelengths other than 494 nm, two phases of absorbance change were observed and the apparent rate constant for each phase was identical to those of the absorbance changes at 494 nm (data not shown). We measured the amplitude of the absorption changes in the presence of 10 mM HOAsp at various wavelengths with 5−10 nm intervals. The absorbance change during the fast phase, ΔA^{fast} (corrected for absorption changes during the dead time), during the slow phase, ΔA^{slow}, and the absorbance at equilibrium, A^{eq}, can be expressed using the molar absorptivity of the reaction intermediates, ϵ^{E_L}, ϵ^{ES_1}, ϵ^{ES_2}, and ϵ^{ES_3}, and the kinetic parameters as follows:

$$\frac{A^{eq} - \Delta A^{slow} - \Delta A^{fast}}{[E_t]} = \epsilon^{E_L}\left(1 - \frac{[S]}{L}\right) + \epsilon^{ES_1}\frac{[S]}{L} \quad (5)$$

$$\frac{A^{eq} - \Delta A^{slow}}{[E_t]} = \epsilon^{E_L}\left(1 - \frac{[S]}{M} - \frac{k_{+2}}{k_{-2}}\frac{[S]}{M}\right) + \epsilon^{ES_1}\frac{[S]}{M} + \epsilon^{ES_2}\frac{k_{+2}}{k_{-2}}\frac{[S]}{M} \quad (6)$$

[3] Equation 3 is the same as equation 38a in Hammes and Schimmel (1970). Equation 4 is derived from the equation for $1/\tau_4$ in Hammes and Schimmel (1966) under the condition that both the accumulation of X_1 and the dissociation of X_4 into C and D are negligible, i.e., $k_{-1} \gg k_1(A + B)$, $k_2 \gg k_{-2}$, and $k_{-5}(C + D) \gg k_5$. The dissociation constant for $A + B \rightleftarrows X_2$ is $k_{-1}k_{-2}/k_1k_2$. (The names of the reaction components and the rate constants are those used in the reference.)

$$\frac{A^{eq}}{[E_t]} = \epsilon^{E_L}\left(1 - \frac{[S]}{N} - \frac{k_{+2}}{k_{-2}}\frac{[S]}{N} - \frac{k_{+2}}{k_{-2}}\frac{k_{+3}}{k_{-3}}\frac{[S]}{N}\right) + \epsilon^{ES_1}\frac{[S]}{N} + \epsilon^{ES_2}\frac{k_{+2}}{k_{-2}}\frac{[S]}{N} + \epsilon^{ES_3}\frac{k_{+2}}{k_{-2}}\frac{k_{+3}}{k_{-3}}\frac{[S]}{N} \quad (7)$$

where

$$L = K_S^{Am} + [S] \qquad M = K_S^{Am} + \left(1 + \frac{k_{+2}}{k_{-2}}\right)[S]$$

$$N = K_S^{Am} + \left(1 + \frac{k_{+2}}{k_{-2}} + \frac{k_{+2}}{k_{-2}}\frac{k_{+3}}{k_{-3}}\right)[S]$$

and $[E_t]$ denotes the total enzyme concentration. These equations show the apparent molar absorptivity of the enzyme just after the encounter of E_L and HOAsp (eq 5), that after the fast phase (eq 6), and that at equilibrium (eq 7), respectively. They were obtained based on the assumption that the reaction reaches a rapid equilibrium between the intermediates at each point on the time axis described above: E_L and ES_1 for eq 5; E_L, ES_1, and ES_2 for eq 6; E_L, ES_1, ES_2, and ES_3 for eq 7. The values of K_S^{Am}, k_{+2}, k_{-2}, k_{+3}, k_{-3}, and ϵ^{E_L} are already known (see the above discussion and Figure 1A). Therefore, we can calculate the values of ϵ^{ES_1}, ϵ^{ES_2}, and ϵ^{ES_3} at variable wavelengths using eqs 5−7. The obtained ϵ values were plotted versus the wavelength (Figure 4). The plots showed the spectra of the individual intermediates; ES_2 showed an intense absorption at around 494 nm with a shoulder at around 460 nm, whereas ES_1 and ES_3 had absorption bands at 350 and 330 nm, respectively, and had no absorption at around 494 nm. Therefore, we can conclude that only ES_2 represents the quinonoid intermediate. The spectra of WT AspAT with high concentrations of HOAsp (Figure 1A) are considered to be mixtures of the spectra of ES_2 and ES_3; these two species are responsible for the 494- and 330-nm absorption, respectively. The $\epsilon_{494}^{ES_2}$ value, i.e., the molar absorptivity of ES_2 at 494 nm, was determined to be 45 300 ± 500 M^{-1} cm^{-1}. This value can be compared to the value of 41 000 M^{-1} cm^{-1} which was deduced for the quinonoid intermediate of glycine hydroxymethyltransferase (Ulevitch & Kallen, 1977) and the value of 46 900 M^{-1} cm^{-1} for the quinonoid complex of tryptophanase with alanine (Metzler et al., 1991). The spectrum of ES_1 is considered to be that of the deprotonated aldimine (Kallen et al., 1985) and may represent the aldimine formed between HOAsp and WT AspAT. On the other hand, the spectrum of ES_3 can represent a variety of structures, such as the ketimine and the carbinolamine (Kallen et al., 1985). We will discuss this later in the Discussion.

As the 494-nm absorption was ascribed solely to ES_2, the ΔA_{494}^{fast} and the ΔA_{494}^{slow} values can be expressed using eqs 5−7 as follows:

$$\frac{\Delta A_{494}^{fast}}{[E_t]} = \epsilon_{494}^{ES_2}\frac{k_{+2}}{k_{-2}}\frac{[S]}{M} \quad (8)$$

$$\frac{\Delta A_{494}^{slow}}{[E_t]} = \epsilon_{494}^{ES_2}\frac{k_{+2}}{k_{-2}}\left(\frac{[S]}{N} - \frac{[S]}{M}\right) \quad (9)$$

These equations were obtained by taking the difference between eqs 5 and 6 (yielding eq 8), and that between eqs 6 and 7 (yielding eq 9), at 494 nm. The equations were simplified to the above forms, because $\epsilon_{494}^{E_L} = \epsilon_{494}^{ES_1} = \epsilon_{494}^{ES_3} = 0$. The experimental data were fitted well to theoretical lines expressed by eqs 8 and 9 (Figure 5). This supported the validity of the values for the kinetic parameters and the reaction scheme (eq 1).

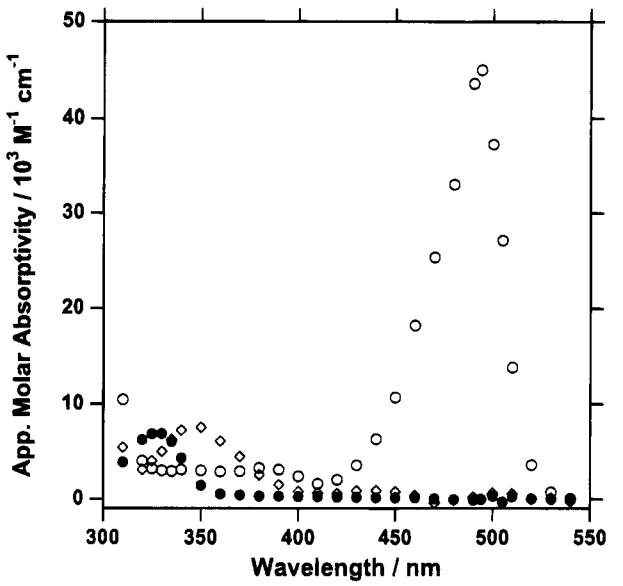

FIGURE 4: Absorption spectra of the intermediates formed by the reaction of WT AspAT with HOAsp. WT AspAT (34.0 μM) was reacted with 10 mM HOAsp, and the absorbance changes during the fast phase, ΔA^{fast}, and the slow phase, ΔA^{slow}, were measured at 5−10 nm intervals. The ΔA^{fast} values were corrected for the absorbance change during the dead time. The absorption spectrum of WT AspAT (34.0 μM) in the presence of 10 mM HOAsp was measured for obtaining the A^{eq} values. The values of molar absorptivity of ES_1 (◇), ES_2 (○), and ES_3 (●) were calculated from ΔA^{fast}, ΔA^{slow}, A^{eq} and ϵ^{E_L}, using eqs 5−7, and were plotted versus the wavelength (see text for detail).

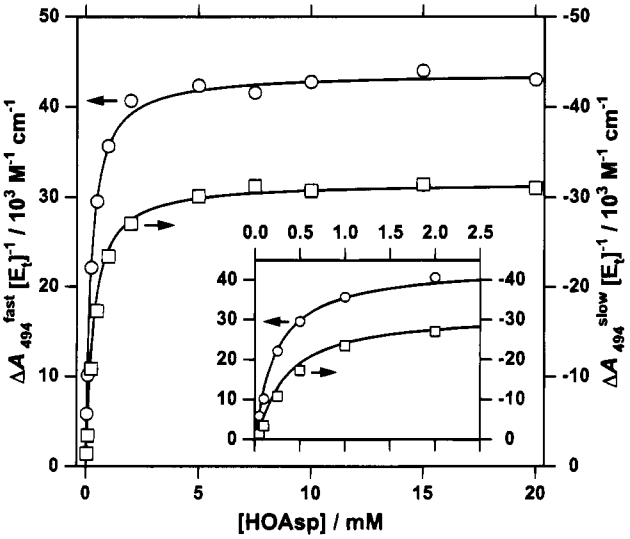

FIGURE 5: Dependency on the HOAsp concentration of the ΔA_{494}^{fast} (○) and ΔA_{494}^{slow} (□) values for the reaction of WT AspAT with HOAsp. WT AspAT (20.0 μM) was reacted with various concentrations of HOAsp (Figure 2), and the absorbance changes during the fast phase and the slow phase were measured. The ΔA_{494}^{fast} values were corrected for the absorbance change during the dead time. The curves are theoretical lines drawn using the obtained parameters and eqs 8 and 9. The inset shows the expansion of the points for low concentrations of HOAsp.

Reaction of HOAsp with Y70F AspAT. The Y70F mutant AspAT has been well characterized (Toney & Kirsch, 1987, 1991; Inoue et al., 1991) and was shown to have almost identical spectroscopic properties to those of WT AspAT. Y70F AspAT had kinetic properties essentially similar to those of WT AspAT; the k_{cat} values of the half transamination reactions were 5−36% of those of WT AspAT, the K_m values for the amino acids were almost unchanged, and the K_m values for the oxo acids were increased by only 10-fold, by the mutation. In spite of this essential similarity in spectroscopic and kinetic properties, Y70F AspAT did not show an intense absorption at around 400−500 nm on the reaction with HOAsp (Figure 1B). Instead, the reaction showed a pattern of spectral changes similar to those of the reactions of WT and Y70F AspATs with aspartate (Inoue et al., 1989; Inoue et al., 1991). These results indicate that the quinonoid intermediate does not accumulate so much during the reaction of Y70F AspAT with HOAsp. However, there was a faint absorption at 494 nm which increased its intensity with increasing concentration of HOAsp (Figure 1B). Such an absorption was completely absent when WT or Y70F AspAT was reacted with aspartate (Inoue et al., 1989; Inoue et al., 1991). When the reaction of HOAsp with Y70F was analyzed in a stopped-flow spectrophotometer, a rapid increase and a slow decrease in the absorbance at 494 nm were observed, although the amplitudes of the absorption changes were much smaller than those of the reaction with WT AspAT. In contrast to the reaction of WT AspAT with HOAsp, dihydroxyfumarate increased the HOAsp-induced absorption at 494 nm of Y70F AspAT (data not shown), indicating that dihydroxyfumarate increased the concentration of the quinonoid intermediate by preventing the dissociation of ES_3 into E_M and OG. This is considered to arise from the low affinity of the PMP form of Y70F AspAT for OG. There was no difference between the data in the presence of 5 mM dihydroxyfumarate and those in the presence of 10 mM dihydroxyfumarate (data not shown), showing that the concentration of 5 mM of dihydroxyfumarate is high enough to analyze the data using the scheme shown in eq 1. The reactions in the presence of 5 mM dihydroxyfumarate were analyzed in the same way as the reactions of WT AspAT with HOAsp (Figure 3B), and the kinetic parameters were obtained: $K_S^{Am} = 3.12 \pm 0.57$ mM, $k_{+2} = 42.0 \pm 1.3$ s^{-1}, $k_{-2} = 310 \pm 2$ s^{-1}, $k_{+3} = 3.49 \pm 0.26$ s^{-1}, and $k_{-3} = 0.568 \pm 0.003$ s^{-1}. From the amplitude of the absorption changes (data not shown), we obtained the value of $\epsilon_{494}^{ES_2} = 40\,000 \pm 7000$ M^{-1} cm^{-1} for the HOAsp complex of Y70F AspAT. The relatively less accurate $\epsilon_{494}^{ES_2}$ value is due to the fact that, during the reaction of Y70F AspAT with HOAsp, the equilibrium between ES_1 and ES_2 is shifted toward the formation of ES_1 ($k_{-2} > k_{+2}$), and consequently the amplitudes of the absorption changes in both the fast and the slow phases were too small to derive a reliable value for $\epsilon_{494}^{ES_2}$. We, therefore, used the value for the HOAsp complex of WT AspAT (45 300 M^{-1} cm^{-1}) in the following calculations.

Equilibrium of the Half-Reaction of the Wild-Type and Y70F AspATs with HOAsp. The kinetic parameters obtained above allows calculation for most part of the free energy profiles (Fersht, 1987) for the reactions of WT and Y70F AspATs with HOAsp. For each reaction, the Gibbs free energy levels of ES_1, ES_2 (the quinonoid intermediate), and ES_3 were calculated. In order to complete the energy profiles, the energy level of E_M was required. This could be obtained from the equilibrium constant $K_{eq}^{HOAsp-OG} = [E_M]_{eq}[OG]_{eq}/([E_L]_{eq}[HOAsp]_{eq})$ for each reaction. We analyzed the data in Figure 1B using the above kinetic parameters in order to calculate the equilibrium constant for the reaction of Y70F AspAT with HOAsp. For each spectrum, E_L, ES_1, ES_2, ES_3, and E_M exist as an equilibrium mixture. The value of $[ES_2]_{eq}$ can be obtained from the values of $\epsilon_{494}^{ES_2}$ and A_{494}. The values of $[ES_1]_{eq}$ and $[ES_3]_{eq}$ were calculated using the values of $[ES_2]_{eq}$, k_{+2}, k_{-2}, k_{+3}, and k_{-3}. The value of $[E_L]_{eq}$ can be obtained from the relation $K_S^{Am} = ([HOAsp_t] + [E_L]_{eq} - [E_t])[E_L]_{eq}/[ES_1]_{eq}$, where $[HOAsp_t]$ is the total HOAsp concentration added to the solution. The value of $[E_M]_{eq}$ was then estimated using the equation $[E_t] = [E_L]_{eq} + [ES_1]_{eq} + [ES_2]_{eq} + [ES_3]_{eq} + [E_M]_{eq}$. Finally, the equilibrium constant was obtained by the equation:

$$K_{eq}^{HOAsp-OG} = \frac{[E_M]_{eq}^2}{[E_L]_{eq}([HOAsp_t] + [E_L]_{eq} - [E_t])} \quad (10)$$

Here $[OG]_{eq}$ was assumed to be equal to $[E_M]_{eq}$, since the oxo acid and the PMP form enzyme were expected to be formed in equal amounts. The results of the calculation is shown in Table 1. We chose the concentrations of HOAsp which produced a significant absorption at 494 nm, in order to perform accurate calculations. The K_{eq} values calculated for the 0.861, 1.80, and 4.07 mM concentrations of HOAsp were 0.115, 0.103, and 0.101, respectively. We used the average of the latter two values, 0.102, in the following calculations.

Table 1: Estimated Concentrations of the Intermediates Present in the Equilibrium Mixture Formed from Y70F AspAT and HOAsp and the Calculated Equilibrium Constant[a]

$[HOAsp_t]$ (mM)	$[ES_2]$ (μM)	$[ES_1]$ (μM)	$[E_L]$ (μM)	$[ES_3]$ (μM)	$[E_M]$ (μM)	K_{eq}
0.861	0.33	2.43	9.18	1.99	29.57	0.115
1.80	0.43	3.15	5.57	2.66	31.69	0.103
4.07	0.49	3.59	2.78	3.03	33.61	0.101

[a] The concentration of each intermediate present in the equilibrium mixtures of Figure 1B was calculated using the values of A_{494}, $\epsilon_{494}^{ES_2}$, and the kinetic parameters obtained from kinetic analysis of the reaction of Y70F AspAT with HOAsp. The method of calculation was described in the text. The enzyme concentration was 43.5 μM. The equilibrium constant for the reaction (K_{eq}) was calculated using eq 10.

We sought to obtain the K_{eq} value for the reaction of WT AspAT with HOAsp in a similar way as above. However, calculation of the concentrations of each intermediate showed that the amounts of E_M were too small to be used for accurately calculating the K_{eq} values using eq 10. The K_{eq} value for the reaction of HOAsp with WT AspAT was, therefore, estimated by the following relationship:

$$K_{eq}^{WT,HOAsp-OG} = K_{eq}^{Y70F,HOAsp-OG} \frac{K_{eq}^{WT,Asp-OA}}{K_{eq}^{Y70F,Asp-OA}} \quad (11)$$

Since the values of $K_{eq}^{WT,Asp-OA}$ and $K_{eq}^{Y70F,Asp-OA}$, i.e., the equilibrium constants for the aspartate−oxalacetate (Asp−OA) reactions with WT and Y70F AspATs, are already

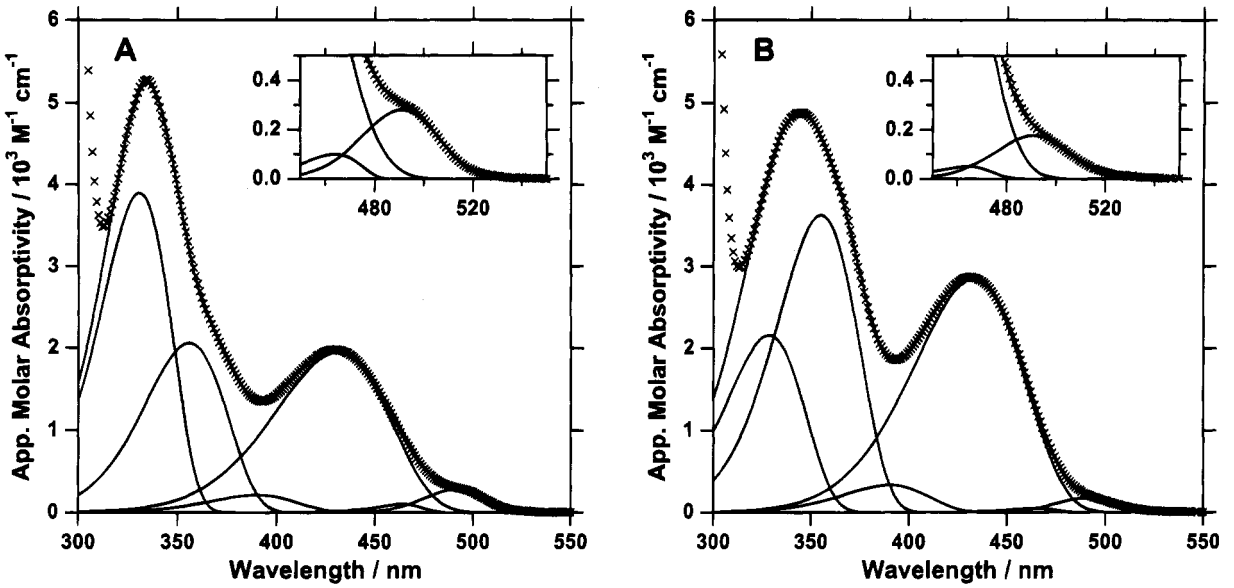

FIGURE 6: Absorption spectra of WT (A) and Y70F (B) AspATs in the presence of 40 mM aspartate and 0.5 mM (WT) or 5 mM (Y70F) oxalacetate. The enzyme concentrations were 80.0 μM. The spectra were taken in 50 mM HEPES−NaOH buffer, pH 8.0, containing 0.1 M KCl, at 25 °C. The spectra between 320 and 550 nm have been fit with six lognormal distribution curves (see Materials and Methods), which are denoted by the solid lines. The summation curves pass very close to the experimental points (×). The inset in each panel shows the expansion of the curves between 450 and 550 nm. The rightmost band in each panel represents the quinonoid intermediate, and the value of the height was used to estimate the concentration of the species (see text for detail).

known to be 0.00535 and 0.0139 (Kuramitsu et al., 1990; Inoue et al., 1991), respectively, the value of $K_{eq}^{WT,HOAsp-OG}$ was calculated to be 0.0393.

Concentration of the Quinonoid Intermediates during the Reaction of WT and Y70F AspATs with Aspartate. Although kinetic analyses of the HOAsp−OG reactions of WT and Y70F AspATs as described above gave parameters for the reaction steps flanking the quinonoid intermediate, the corresponding Asp−OA reactions could not be similarly analyzed, for they do not show significant absorption changes at around 500 nm (Kuramitsu et al., 1990; Inoue et al., 1991). We estimated the equilibrium concentration of the quinonoid intermediate by static spectroscopic analysis of WT and Y70F AspATs in the presence of saturating amounts of Asp and OA (Figure 6; see Metzler & Metzler, 1987). Both spectra showed a small but significant absorption at around 500 nm, indicating the presence of the quinonoid intermediate. The spectra were resolved into lognormal curves (Figure 6) according to the method of Metzler and Metzler (1987). From the apparent molar absorptivity of the peak of the 494-nm components, the concentrations of the quinonoid species were calculated. The ϵ_{494} value for the quinonoid intermediate formed during the reaction of aspartate with AspAT could not be obtained because of the reasons described above, and we used the value of $\epsilon_{494}^{ES_2} = 45\,300$ M^{-1} cm^{-1}, which had been determined for the quinonoid structure produced from HOAsp and WT AspAT, for the calculation. The amounts of the quinonoid intermediates are 0.623% and 0.382% of the total WT AspAT and Y70F AspAT, respectively, in the presence of saturating amounts of aspartate and oxalacetate. Together with the values of the kinetic parameters for the reaction of WT and Y70F AspAT with aspartate and oxalacetate (Kuramitsu et al., 1990; Inoue et al., 1991), the values of the equilibrium constant, $K_{eq}^{ES_1-ES_2} = [ES_2]_{eq}/[ES_1]_{eq}$, were determined to be 0.0106 for WT AspAT and 0.00423 for Y70F AspAT, respectively. The values of the parameters obtained above were used to draw free energy profiles of the reactions of WT and Y70F AspAT with aspartate and HOAsp (Figure 7).

DISCUSSION

From the above kinetic and spectroscopic analysis of the reactions of HOAsp with WT and Y70F AspATs, it is evident that the quinonoid intermediate (ES_2) is stabilized by the interaction of the β-hydroxy group of HOAsp with the phenolic hydroxy group of Tyr70, as has been suggested by Taylor and Metzler (1990). For detailed thermodynamic discussions of the stabilization of the intermediate structures, the free energy profiles for these reactions are of great use. The energy profiles were drawn using the previously determined kinetic parameters (Kuramitsu et al., 1990; Inoue et al., 1991) and the kinetic parameters obtained in this study (Figure 7). The energy level of ES_2 in the Asp−OA reaction was slightly increased (2.6 kJ mol^{-1}) by Y70F mutation (Figure 7). Therefore, the hydroxy group of Tyr70 has a fine-tuning rather than essential role in the stabilization of the quinonoid intermediates of normal substrates as has been suggested by Toney and Kirsch (1991). For WT AspAT (Figure 7A), comparison of the profiles of the HOAsp−OG reaction and the Asp−OA reaction showed that incorporation of a hydroxy group into C^{β} of the substrate aspartate stabilizes the quinonoid intermediate by 18.5 kJ mol^{-1} (Figure 7A). When we made a similar comparison in Y70F AspAT, we found that the free energy of stabilization is 9.8 kJ mol^{-1} (Figure 7B). Then we concluded that a significant part of the stabilization of the quinonoid structure by the β-hydroxy group is provided by the interaction of the β-hydroxy group with the phenolic hydroxy group of Tyr70. In order to know the mechanism of stabilization of the quinonoid intermediate by the hydroxy groups of HOAsp and Tyr70, model building of the quinonoid intermediate structure produced from HOAsp and PLP in WT AspAT was attempted (Figure 8) using the coordinates of the closed form of *E. coli* AspAT complexed with 2-methylaspartate (Oka-

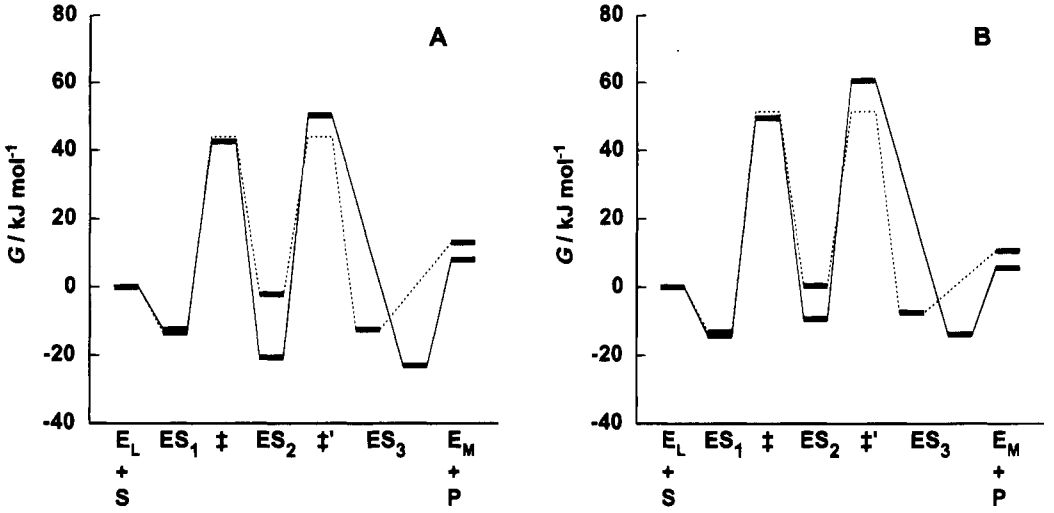

FIGURE 7: Free energy profiles for the reaction of WT (A) and Y70F (B) AspATs with HOAsp (solid lines) and aspartate (dashed lines). Symbols are the same as those used in eqs 1 and 2. For the reactions with HOAsp, the free energy values for ES_1, ES_2, ES_3, and the transition states (‡ and ‡′) connecting them, relative to that of E_L + S, were calculated from the kinetic parameters shown in eq 1 according to the method of Fersht (1987). The free energy levels of E_M were estimated from the K_{eq} values for the reactions (see text). For the reactions with aspartate, the energy levels for the intermediates except for those of ES_2 were taken from previous studies (Kuramitsu et al., 1990; Inoue et al., 1991), and the energy levels of ES_2 were calculated from the equilibrium constants for $ES_2 \rightleftarrows ES_1$ (see text). There are two transition states (‡ and ‡′) for the reaction with aspartate, but only one energy level of the transition state is known because the value was obtained from the kinetic parameters (k_{cat} and K_m) for the half-reactions (Kuramitsu et al., 1990; Inoue et al., 1991). The same height of the energy levels of ‡ and ‡′ expressed by the dashed lines in each panel should be thus considered to indicate that the energy level corresponds to only one of the two transition states, ‡ or ‡′. We have tentatively assigned the ketimine structure for ES_3 in the Asp−OA reactions and the carbinolamine structure for ES_3 in the HOAsp−OG reactions (see text). Therefore, the energy levels for ES_3 of the Asp−OA reaction and the HOAsp−OG reaction are shown at different positions in each panel.

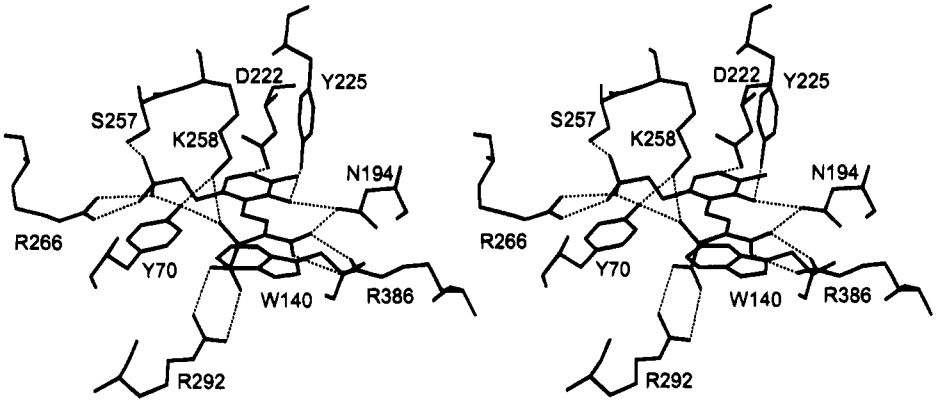

FIGURE 8: Stereo drawing of a possible structure of the quinonoid intermediate of HOAsp and PLP modeled on the closed conformation of *E. coli* WT AspAT. *E. coli* AspAT complexed with 2-methylaspartate (Okamoto et al., 1994; Protein Data Bank identification code 1ART) was used as the template. 2-Methylaspartate was modified to 3-hydroxyaspartate, and bond orders of the complex with PLP were adjusted to a quinonoid structure. The geometry of the HOAsp−PLP quinonoid complex was optimized by a MOPAC (QCPE Program 141) calculation using PM3 Hamiltonian. The resultant bond lengths and angles were fixed. The C5−C5′, C5′−O5′, and O5′−P bonds of the coenzyme and the bonds around substrate C^{β} were allowed to rotate, while the torsion angles around all other bonds were fixed in the subsequent calculation. Energy minimization was carried out using Quanta/CHARMm (version 4.0/2.2, Molecular Simulations Inc., Waltham, MA). The atoms of the HOAsp−PLP complex except for the phosphate group and the side chains of Arg292, Arg386, Asn194, Trp140, Lys258, and Tyr70 were allowed to move, while the positions of all other atoms were fixed. As the result, the two carboxylate groups of HOAsp were able to form hydrogen bonds with the two arginyl residues, Arg292 and Arg386. This was made possible by a 12° torsional rotation around C5−C5′ of the coenzyme. The O^{η} atom of Tyr70 and the N^{ζ} atom of Lys258 moved toward the $O^{\gamma 1}$ atom of the β-hydroxy group of HOAsp by 0.35 and 0.60 Å, respectively. Possible hydrogen bonds are drawn by dashed lines. The atomic distances of the hydrogen bonds are as follows: Lys258 N^{ζ}−HOAsp $O^{\gamma 1}$ (hydroxy), 2.5 Å; Lys258 N^{ζ}−Tyr70 O^{η}, 2.5 Å; Tyr70 O^{η}−HOAsp $O^{\gamma 1}$ (hydroxy), 2.5 Å; Tyr70 O^{η}−PLP OP2, 2.7 Å; Arg386 $N^{\eta 1}$−HOAsp OT1 (front), 2.7 Å; Arg386 $N^{\eta 2}$−HOAsp OT2 (back), 2.5 Å; Arg292 $N^{\eta 1}$−HOAsp $O^{\delta 2}$ (front), 3.0 Å; Arg292 $N^{\eta 2}$−HOAsp $O^{\delta 1}$ (back), 2.8 Å; Asn194 $N^{\delta 2}$−HOAsp OT2, 2.6 Å; Asn194 $N^{\delta 2}$−PLP O3′, 2.6 Å; Tyr225 O^{η}−PLP O3′, 3.1 Å; Arg266 $N^{\eta 1}$−PLP OP3, 2.7 Å; Arg266 $N^{\eta 2}$−PLP OP2, 2.8 Å; Ser257 O^{γ}−PLP OP1; 2.9 Å; Asp222 $O^{\delta 1}$−PLP N1, 2.9 Å. The atoms names are those used by Okamoto et al. (1994).

moto et al., 1994). In the energy minimizing model (Figure 8), the α- and β-carboxylate groups of the quinonoid intermediate of HOAsp−PLP complex electrostatically interacts with the guanidinium groups of Arg386 and Arg292 in the same way as the aldimine of 2-methylaspartate−PLP interacts with these arginine residues (Okamoto et al., 1994). The β-hydroxy O ($O^{\gamma 1}$)[4] of HOAsp is within a hydrogen-bonding distance from O^{η} of Tyr70 (Figure 8). In addition, the model showed that N^{ζ} of Lys258 is also close enough to

[4] The hydroxy O atom of HOAsp was named $O^{\gamma 1}$ according to the atom names of threonine.

Chart 1: Intermediate Structures of the HOAsp−PLP Complex in WT AspAT with Possible Hydrogen-Bonding Patterns. (A) The Quinonoid Intermediate. (B) The Ketimine. (C) The Carbinolamine[a]

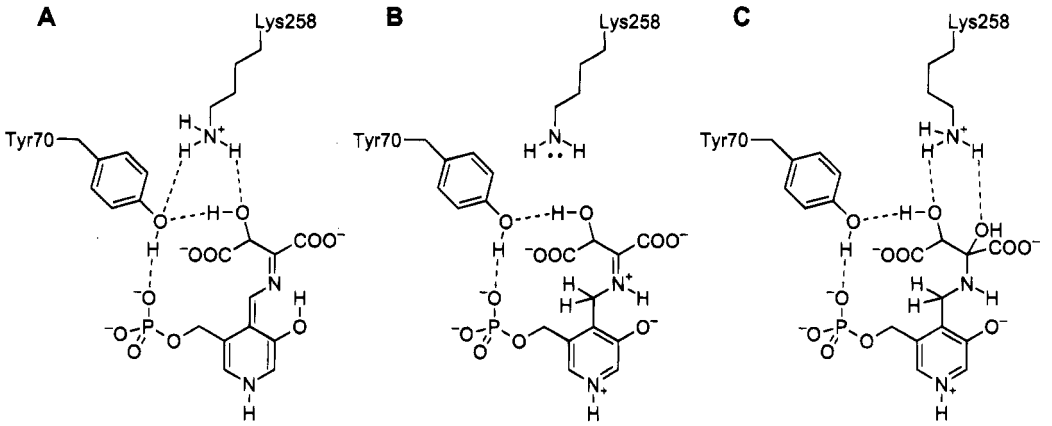

[a] In (A) and (C), the ϵ-amino group of Lys258 is protonated and is involved in the hydrogen-bonding network.

both O^{η} of Tyr70 and $O^{\gamma 1}$ of HOAsp to form a hydrogen-bonding network between Lys258, HOAsp, Tyr70, and the phosphate group of PLP (Figure 8). That the β-hydroxy group of HOAsp can form a hydrogen bond with the ϵ-amino group of Lys258 is in accordance with the observation that, even in Y70F AspAT, the β-hydroxy group stabilizes the quinonoid structure by 9.8 kJ mol^{-1} (Figure 7B). Therefore, the strength of the hydrogen bond formed between the β-hydroxy group of HOAsp and the ϵ-amino group of Lys258 is roughly estimated to be 9.8 kJ mol^{-1}, and that formed between the β-hydroxy group and the hydroxy group of Tyr70 is (18.5 − 9.8) = 8.7 kJ mol^{-1}. A possible hydrogen-bonding pattern is illustrated in Chart 1A. In the quinonoid intermediate, the α-proton is transferred from the PLP−HOAsp complex to the ϵ-amino group of Lys258. As a result, the protonated amino group of Lys258 can donate hydrogen atoms to both the β-hydroxy group of HOAsp and the phenolic hydroxy group of Tyr70. HOAsp donates a hydrogen atom to Tyr70, and Tyr70 to the phosphate group of PLP. The entire hydrogen-bonding network is supposed to be stabilized by mutual compensation of the positive charge of the amino group of Lys258 and the negative charge of the phosphate group of PLP.

In contrast to the case of the quinonoid intermediate, the energy level of ES_1 was essentially unchanged by the incorporation of the β-hydroxy group into the substrate (Figure 7A). We interpreted this observation as follows. In the aldimine, and also in the ketimine structures, the amino group of Lys258 is not protonated (Arnone et al., 1985a). This should make the ϵ-amino group of Lys258 a relatively weak hydrogen donor, and the hydrogen-bonding network, which has been suggested for the quinonoid intermediate (Chart 1A), is less likely to be formed in these structures (for the aldimine see Chart 1B). Therefore, if we assume that ES_1 represents the aldimine, we can explain the observation that ES_1 was not stabilized by the β-hydroxy group.

The energy level of ES_3 in the HOAsp−OG reaction was 10.6 kJ mol^{-1} lower than that of ES_3 in the Asp−OA reaction (Figure 7A). It is hard to explain this observation if we assume that ES_3 represents the ketimine in both the HOAsp−OG and the Asp−OA reactions, because the ketimine is not expected to be stabilized by the β-hydroxy group (see the above discussion). Malashkevich et al. (1993) reported that when chicken mitochondrial AspAT was crystallized in the presence of aspartate or glutamate, the obtained crystal structure was the ketimine. On the other hand, the same group recently found that the crystal of chicken mitochondrial AspAT complexed with HOAsp showed an sp^3-hybridized structure at C^{α} of the HOAsp−PLP complex, suggesting it to be the carbinolamine structure (Genovesio et al., 1994). They considered the reason for the stabilization of the carbinolamine intermediate to be the fact that several hydrogen bonds can be made between the two hydroxy groups at C^{α} and C^{β} of the carbinolamine with the hydroxy group of Tyr70 and the ϵ-amino group of Lys258 (see Chart 1C). Taken together, we consider that ES_3 represents the ketimine in the Asp−OA reaction, and the carbinolamine in the HOAsp−OG reaction. This indicates that the β-hydroxy group of HOAsp stabilizes the carbinolamine. In the carbinolamine structure of the normal substrates, the O atom of the newly formed α-hydroxy group is supposed to make a hydrogen bond to N^{ζ} of Lys258, because the ϵ-amino group of Lys258 is considered to act as a general base catalyst when a water molecule attacks the ketimine to form the carbinolamine (Arnone et al., 1985a). For the reaction of AspAT with HOAsp, we can expect that the protonated ϵ-amino group of Lys258 can make hydrogen bonds to both the α- and β-hydroxy groups of the carbinolamine, thereby forming a hydrogen-bonding network which stabilizes the carbinolamine structure in the HOAsp−OG reaction (Chart 1C). According to this proposal, Figure 7A indicates that the energy level of the ketimine in the Asp−OA reaction is 10.6 kJ mol^{-1} higher than that of the carbinolamine in the HOAsp−OG reaction. The energy level of the carbinolamine in the Asp−OA reaction is difficult to know, but is expected to be greater than that of the ketimine in the Asp−OA reaction. Therefore, the free energy of stabilization of the carbinolamine by incorporating the β-hydroxy group to the substrate aspartate is expected to be greater than 10.6 kJ mol^{-1}. The fact that we cannot accurately determine the energy level of the carbinolamine in the Asp−OA reactions hampers further energetic analysis of the carbinolamine structure. The extent of the involvement of Tyr70 in this stabilization of the carbinolamine is also difficult to estimate, because, at present, we have no crystallographic information about the structure of Y70F AspAT complexed with either aspartate or HOAsp. However, if we assume ES_3 in the HOAsp−OG reaction of Y70F AspAT represents the carbinolamine, we can expect that Tyr70 contributes 9.3 kJ mol^{-1}

to the stabilization of the carbinolamine in the HOAsp−OG reaction, by comparing the energy level of ES_3 in the HOAsp−OG reaction of Y70F AspAT to that of WT AspAT. From the above discussion, we can conclude that the hydrogen-bond network involving the two hydroxy groups of HOAsp and Tyr70 and possibly the amino group of Lys258 stabilizes both the quinonoid and the carbinolamine intermediates.

The importance of Lys258 in the hydrogen-bonding network suggested in this study may be assessed by analyzing the reaction of HOAsp with K258A AspAT. The complex of K258A AspAT with HOAsp showed a spectrum of the external aldimine and no apparent absorption at around 490−500 nm.[5] However, we cannot consider this observation to be proof of the structure shown in Chart 1A. Since Lys258 is known to be a critical catalytic residue that abstracts the proton at C^{α} of substrates (Arnone et al., 1985a), it is possible to consider that Lys258 stabilizes the quinonoid intermediate of the HOAsp−PLP Schiff base without interacting with the hydroxy groups of HOAsp and Tyr70. Nevertheless, the proposal of a hydrogen-bonding network involving the protonated ϵ-amino group of Lys258 can well explain all the results presented in this study and the crystallographic observations on the complex of AspAT with aspartate and HOAsp (Malashkevich et al., 1993; Genovesio et al., 1994).

The present study demonstrated that the stabilization of the quinonoid structure produced by the reaction of WT AspAT with HOAsp is mediated by the interaction of the β-hydroxy group of HOAsp with the active site residues. A hydrogen bond formed between the β-hydroxy group of HOAsp and the phenolic hydroxy group of Tyr70 is important for stabilizing the structure of the quinonoid intermediate, but interactions of the β-hydroxy group of HOAsp with residue(s) other than Tyr70 further stabilize the quinonoid intermediate. We suggest that the ϵ-amino group of Lys258 is responsible for the latter set of interactions. The kinetic analysis also indicated that there is another energetically favorable structure, which is in equilibrium with the quinonoid intermediate. Mechanistic considerations suggested the carbinolamine intermediate for this structure, which is also possibly stabilized by interactions of the β-hydroxy group of HOAsp with Tyr70 and Lys258. These findings provide important implications for the understanding of the mechanism of AspAT and related aminotransferases as follows.

First, the pattern of the hydrogen-bonding network shown in Figure 8 indicates an interaction between the protonated amino group of Lys258 and the phenolic hydroxy group of Tyr70. Although there remains the possibility that this Lys258−Tyr70 interaction is a kind of "artifact" that was brought about by the incorporation of the β-hydroxy group into the substrate, the above model suggests that this interaction can also take place in the normal catalytic reaction of AspAT with aspartate. An energy minimizing model of the quinonoid intermediate of aspartate and PLP in AspAT showed that the distance between N^{ζ} of Lys258 and O^{η} of Tyr70 is 2.6 Å, supporting this hypothesis (data not shown).[6] Through this interaction, O^{η} of Tyr70 can serve as a bridge between the negative charge of the phosphate group of PLP and the positive charge of the protonated ϵ-amino group of Lys258 in the quinonoid intermediate. Although this interaction does not seem to be essential in the normal catalytic reaction, it may account for the observation that the presence of the phenolic hydroxy group of Tyr70 stabilizes the quinonoid intermediate of the Asp−OA reaction by 2.6 kJ mol^{-1} (Figure 7) and enhances the catalytic efficiency (k_{cat}/K_m) by about 1 order of magnitude (Toney & Kirsch, 1987, 1991; Inoue et al., 1991).

Second, the finding that an intermediate (possibly the carbinolamine) other than the quinonoid intermediate accumulates and the concentration of the former exceeds that of the latter indicates that the HOAsp−AspAT complex cannot be treated as a single species. This is especially important when we analyze the spectroscopic data on the HOAsp−AspAT complex, obtained by resonance Raman or NMR spectroscopy, in order to characterize the quinonoid intermediate structure.

Finally, the finding that the β-hydroxy group of HOAsp interacts with the phenolic hydroxy group of Tyr70, and possibly with the ϵ-amino group of Lys258, is of great use in studying the nature of substrate binding to aminotransferases related to AspAT. *E. coli* aromatic amino acid aminotransferase is closely related to AspAT in primary structure, but the crystallographic data are not obtained at present. Because of this, the nature of the binding of the aromatic substrates such as phenylalanine or tyrosine to this enzyme has been controversial (Jäger et al., 1992; Seville et al., 1988). This enzyme reacts with both L-*erythro*-3-hydroxyaspartate and L-*erythro*-3-phenylserine to yield intense absorption bands at around 490−500 nm (Hayashi et al., 1993). Preliminary studies showed that the absorption band produced by either of the 3-hydroxy amino acids is diminished by mutation of Tyr70 to phenylalanine.[5] This indicates that the β-hydroxy (3-hydroxy) groups of L-*erythro*-3-hydroxyaspartate and L-*erythro*-3-phenylserine similarly interact with Tyr70 and suggests a nearly superimposable geometry of these 3-hydroxy amino acids in the enzyme. Analysis of these reactions will provide a detailed understanding of the binding nature of the acidic and the aromatic amino acids within the enzyme and is expected to facilitate the elucidation of the substrate recognition mechanism of the enzyme. This work is now under way in our laboratory.

REFERENCES

Arnone, A., Christen, P., Jansonius, J. N., & Metzler, D. E. (1985a) in *Transaminases* (Christen, P., & Metzler, D. E., Eds.) pp 326−362, John Wiley & Sons, New York, NY.

Arnone, A., Rogers, P. H., Hyde, C. C., Briley, P. D., Metzler, C. M., & Metzler, D. E. (1985b) in *Transaminases* (Christen, P., & Metzler, D. E., Eds.) pp 138−154, John Wiley & Sons, New York, NY.

Danishevsky, A. T., Onnufer, J. J., Petsko, G. A., & Ringe, D. (1991) *Biochemistry 30*, 1980−1985.

Fasella, P., & Hammes, G. G. (1967) *Biochemistry 6*, 1798−1804.

Fersht, A. (1985) *Enzyme Structure and Mechanism*, pp 311−346, W. H. Freeman and Co., New York, NY.

[5] Hayashi, Kagamiyama, et al., unpublished results.

[6] The energy minimization was carried out in the same way as described in the legend of Figure 8, except the β-hydroxy group was omitted from the quinonoid structure. After the minimization, O^{η} of Tyr70 and N^{ζ} of Lys258 moved forward (in Figure 8) by 0.4 and 3.1 Å, respectively, from the positions of these atoms in the WT AspAT−2-methylaspartate complex. The distance between O^{η} of Tyr70 and OP2 of PLP was 3.0 Å.

Genovesio, J.-C., von Stosch, A., Malashkevich, V. N., Toney, M. D., & Jansonius, J. N. (1994) in *Abstracts of the 9th Meeting of Vitamin B6 and Carbonyl Catalysis and the 3rd Symposium of PQQ and Quinoproteins*, Capri, Italy, p 114.

Hammes, G. G., & Schimmel, P. R. (1966) *J. Phys. Chem. 70*, 2319−2324.

Hammes, G. G., & Haslam, J. L. (1969) *Biochemistry 8*, 1591−1598.

Hammes, G. G., & Schimmel, P. R. (1970) in *The Enzymes* (Boyer, P. D., Ed.) pp 67−114, Academic Press, New York, NY.

Harruff, R. C., & Jenkins, W. T. (1978) *Arch. Biochem. Biophys. 188*, 37−46.

Hayashi, H., Inoue, K., Nagata, T., Kuramitsu, S., & Kagamiyama, H. (1993) *Biochemistry 32*, 12229−12239.

Inoue, K., Kuramitsu, S., Okamoto, A., Hirotsu, K., Higuchi, T., & Kagamiyama, H. (1991) *Biochemistry 30*, 7796−7801.

Inoue, Y., Kuramitsu, S., Inoue, K., Kagamiyama, H., Hiromi, K., Tanase, S., & Morino, Y. (1989) *J. Biol. Chem. 264*, 9673−9681.

Jäger, J., Solmajer, T., & Jansonius, J. N. (1992) *FEBS Lett. 306*, 234−238.

Jäger, J., Moser, M., Sauder, U., & Jansonius, J. N. (1994) *J. Mol. Biol. 239*, 285−305.

Jansonius, J. N., Eichele, G., Ford, G. C., Picot, D., Thaller, C., & Vincent, M. (1985) in *Transaminases* (Christen, P., & Metzler, D. E., Eds.) pp 109−137, John Wiley & Sons, New York, NY.

Jenkins, W. T. (1961) *J. Biol. Chem. 234*, 1121−1125.

Kallen, R. G., Korpela, T., Martell, A. E., Matsushima, Y., Metzler, C. M., Metzler, D. E., Morozov, Yu. V., Ralston, I. M., Savin, F. A., Torchinsky, Yu. M., & Ueno, H. (1985) in *Transaminases* (Christen, P., & Metzler, D. E., Eds.) pp 37−108, John Wiley & Sons, New York, NY.

Kamitori, S., Okamoto, A., Hirotsu, K., Higuchi, T., Kuramitsu, S., Kagamiyama, H., Matsuura, Y., & Katsube, Y. (1990) *J. Biochem. 108*, 175−184.

Kirsch, J. F., Eichele, G., Ford, G. C., Vincent, M. G., Jansonius, J. N., Gehring, H., & Christen, P. (1984) *J. Mol. Biol. 174*, 497−525.

Kuramitsu, S., Hiromi, K., Hayashi, H., Morino, Y., & Kagamiyama, H. (1990) *Biochemistry 29*, 5469−5476.

Malashkevich, V. N., Toney, M. D., & Jansonius, J. N. (1993) *Biochemistry 32*, 13451−13462.

Metzler, C. M. & Metzler, D. E. (1987) *Anal. Biochem. 166*, 313−327.

Metzler, C. M., Viswanath, R., & Metzler, D. E. (1991) *J. Biol. Chem. 266*, 9374−9381.

Okamoto, A., Higuchi, T., Hirotsu, K., Kuramitsu, S., & Kagamiyama, H. (1994) *J. Biochem. 116*, 95−107.

Ovchinnikov, Yu., Egorov, C. A., Aldanova, N. A., Feigina, M. Yu., Lipkin, V. M., Abdulaev, N. G., Grishin, E. V., Kiselev, A. P., Modyanov, N. N., Braunstein, A. E., Polyanovsky, O. L., & Nosikov, V. V. (1973) *FEBS Lett. 29*, 31−34.

Seville, M., Vincent, M. G., & Hahn, K. (1988) *Biochemistry 27*, 8344−8349.

Taylor, J. E., & Metzler, D. E. (1990) in *Vitamin B_6* (Dakshinamurti, K., Ed.) Annals of the New York Academy of Sciences, Vol. 585, pp 58−67, New York Academy of Sciences, New York, NY.

Toney, M. D., & Kirsch, J. F. (1987) *J. Biol. Chem. 262*, 12403−12405.

Toney, M. D., & Kirsch, J. F. (1991) *Biochemistry 30*, 7456−7461.

Tonomura, B., Ohnishi, M., Nakatani, H., Yamaguchi-Itoh, J., & Hiromi, K. (1978) *Anal. Biochem. 84*, 370−383.

Ulevitch, R. J., & Kallen, R. G. (1977) *Biochemistry 16*, 4350−4354.

BI9502506